

See discussions, stats, and author profiles for this publication at: <https://www.researchgate.net/publication/275223279>

# Sticking and splashing in yield-stress fluid drop impacts on coated surfaces

Article in Physics of Fluids · April 2015

DOI: 10.1063/1.4916620

---

CITATIONS

42

READS

441

4 authors, including:



Marc Deetjen

Stanford University

7 PUBLICATIONS 112 CITATIONS

[SEE PROFILE](#)



Randy H Ewoldt

University of Illinois, Urbana-Champaign

189 PUBLICATIONS 7,913 CITATIONS

[SEE PROFILE](#)



## Sticking and splashing in yield-stress fluid drop impacts on coated surfaces

Brendan C. Blackwell, Marc E. Deetjen, Joseph E. Gaudio, and Randy H. Ewoldt

Citation: Physics of Fluids (1994-present) **27**, 043101 (2015); doi: 10.1063/1.4916620

View online: <http://dx.doi.org/10.1063/1.4916620>

View Table of Contents: <http://scitation.aip.org/content/aip/journal/pof2/27/4?ver=pdfcov>

Published by the AIP Publishing

---

### Articles you may be interested in

[Colloidal microstructure effects on particle sedimentation in yield stress fluids](#)

J. Rheol. **57**, 1761 (2013); 10.1122/1.4824471

[Strong squeeze flows of yield-stress fluids: The effect of normal deviatoric stresses](#)

J. Rheol. **57**, 719 (2013); 10.1122/1.4794912

[Rayleigh-Bénard convection for viscoplastic fluids](#)

Phys. Fluids **25**, 023101 (2013); 10.1063/1.4790521

[Boundary layer in pastes—Displacement of a long object through a yield stress fluid](#)

J. Rheol. **56**, 1083 (2012); 10.1122/1.4720387

[Drag force on a sphere in steady motion through a yield-stress fluid](#)

J. Rheol. **51**, 125 (2007); 10.1122/1.2401614

---



# Sticking and splashing in yield-stress fluid drop impacts on coated surfaces

Brendan C. Blackwell, Marc E. Deetjen, Joseph E. Gaudio,  
and Randy H. Ewoldt<sup>a)</sup>

*Department of Mechanical Science and Engineering, University of Illinois  
at Urbana-Champaign, Urbana, Illinois 61801, USA*

(Received 4 August 2014; accepted 14 February 2015; published online 6 April 2015)

Yield-stress fluids, including gels and pastes, are effectively fluid at high stress and solid at low stress. In liquid-solid impacts, the fluid motion can be halted by the yield stress at different points of the event, and these fluids can therefore stick and accumulate where they impact, motivating several applications of these rheologically complex materials. Here, we use high-speed imaging to experimentally study liquid-solid impact of yield-stress fluids on pre-coated horizontal surfaces. With a pre-coating of the same material, we can observe large long-lifetime ejection sheets with redirected momentum which extend away from the impact location. Under critical splash conditions, sheet breakup occurs and ejected droplets can be nonspherical and threadlike due to the inability of capillary stresses to deform material above a certain lengthscale. By varying the droplet size, impact velocity, surface coating thickness, and rheological material properties, we develop appropriate dimensionless parameters and present a low-dimensional regime map of impact behaviors. © 2015 AIP Publishing LLC. [<http://dx.doi.org/10.1063/1.4916620>]

## I. INTRODUCTION

Yield-stress fluids are pervasive in industrial applications such as food processing, agriculture, grease lubrication, and manufacturing.<sup>1</sup> Many of these applications (including fire suppression and coating processes) involve fluid droplets impacting surfaces. Significant study has already been devoted to the impact of yield-stress fluid droplets onto dry surfaces.<sup>2–7</sup> In applications such as coating processes, while some droplets hit dry surfaces, many impact a surface that is already coated in a layer of the impacting material. In Newtonian fluids, it has been observed that a drop hitting a wet surface can coalesce with the wetting liquid or splash depending upon the physical parameters,<sup>8</sup> and some theoretical and mathematical characterizations of this transition have been successful.<sup>9–14</sup> Other work has also broken the impact event types into more categories.<sup>8,15,16</sup> While Newtonian fluid drops impacting wetted surfaces have been studied, the problem of yield-stress drops impacting pre-coated surfaces has not yet been addressed.

The problem of characterizing impact onto a pre-coated surface is more complex than that of a dry surface. Although the variable of surface hydrophobicity may be negligible, since the surface is completely wetted prior to impact, an extra variable—the thickness of the pre-coating layer—affects the dynamics. In addition, the drop can form an ejection sheet extending above and away from the surface that can deform in three dimensions and break up in multiple ways. Drops on dry surfaces tend to deform primarily in the plane of the surface and rarely experience the type of dramatic splash events seen with a pre-coated surface.

Here, we explore the transition from sticking behavior to splashing behavior when a drop of a yield-stress fluid impacts a surface that is pre-coated with a uniform layer of the impacting material. First, we detail our experimental material and apparatus, including a new device to create spherical

<sup>a)</sup>Author to whom correspondence should be addressed. Electronic mail: [ewoldt@illinois.edu](mailto:ewoldt@illinois.edu)

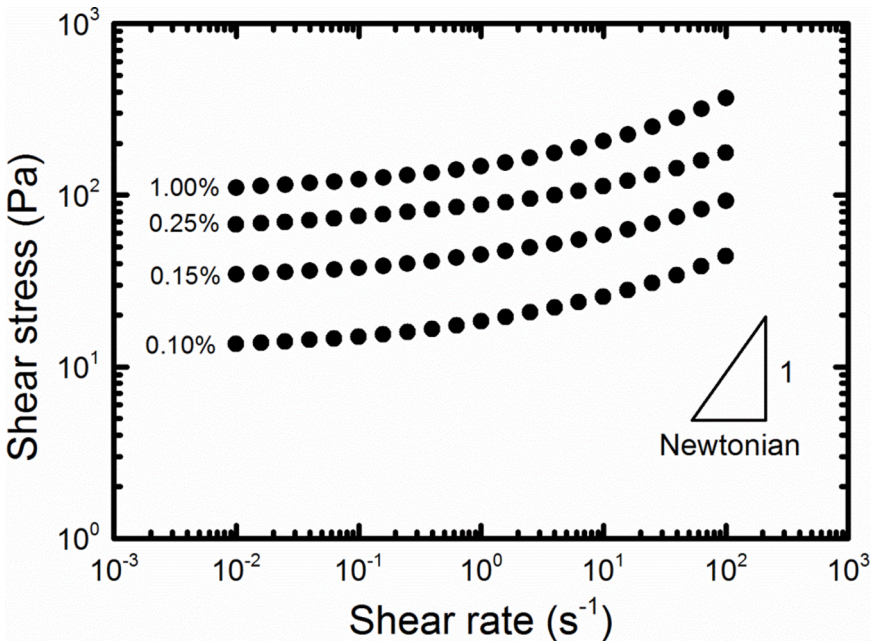


FIG. 1. Steady-state flow curves for four concentrations (wt. %) of Carbopol in water (pH 7).

droplets of yield-stress fluids (Sec. II). We then present a number of example drop impacts and proceed to observe and classify the different types of impact behavior as a function of four dimensional input variables (Sec. III). Finally, we discuss nondimensionalization of the problem and present the impact regimes as a function of the relevant dimensionless groups (Sec. IV), reducing the parameter space from four parameters to one parameter to distinguish different splash regimes.

## II. EXPERIMENTAL SETUP

For this first exploration into this experimental space, we use a well-studied model yield-stress fluid, an aqueous solution of Carbopol 940, neutralized to a pH of 7. Carbopol is a polymer microgel, a crosslinked polymer particle. Particles in solution form a jammed system that exhibits a yield stress when the concentration is sufficiently high. Carbopol suspensions are soft glassy materials that have a very short thixotropic restructuring time (on the order of 1 s).<sup>17</sup> Figure 1 shows the steady-shear flow curves of the four concentrations of Carbopol used in this study. Data shown are sweeps from high rate to low rate; hence, the measurement results in a dynamic yield stress. Rheological characterization was performed on a TA Instruments DHR-3 rotational rheometer using a parallel disk geometry with adhesive-backed sandpaper to prevent slip (tests were performed at multiple gaps to verify the absence of slip).<sup>18</sup> Parallel disk corrections were used to identify the true shear stress.<sup>19</sup> The curves can be reasonably approximated by fitting a two parameter Bingham model, characterizing each concentration with a yield stress and an infinite shear viscosity. Better fits can be achieved with more parameters, but in consideration of easily interpreting results, we will proceed with a two parameter fit (we will discuss this further in Sec. IV).

One issue in studying drops of yield-stress fluids is that the presence of a yield stress allows drops to stably maintain non-uniform shapes (e.g., Refs. 2–4), and the shape of a drop can affect impact dynamics. Spherical drops lend greater repeatability and simpler physics to the experimental process. As such, we designed and fabricated the device diagramed in Figure 2, which employs two counter-rotating quarter spheres with hydrophobic coatings to carve spheres of gel. The improvement in shape compared to a drop extruded from a syringe is shown in Figure 3.

We perform impact experiments by positioning the spherical droplet mechanism above a horizontal glass plate coated with a layer of the same material as the drop, as drawn in Figure 4. The material was centrifuged to remove air bubbles, then applied to the surface, and spread to the target

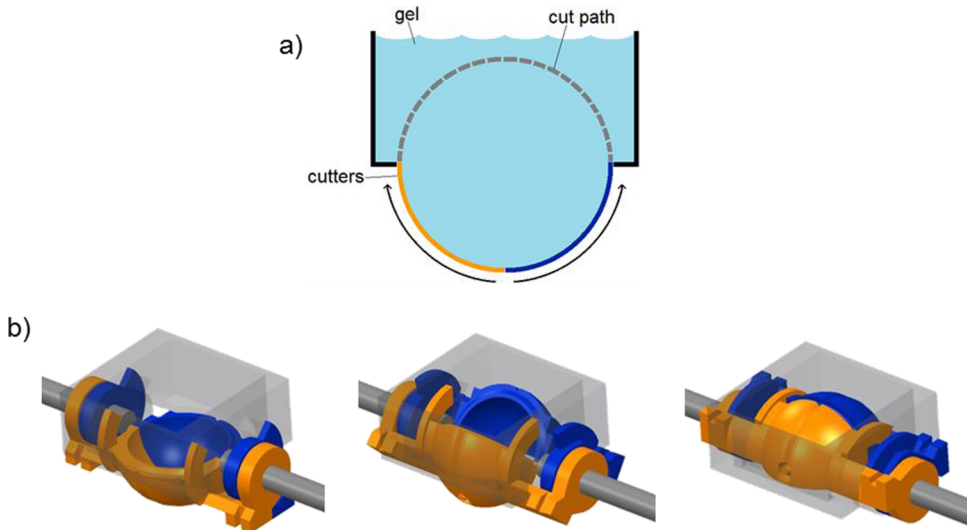


FIG. 2. Spherical droplet cutting mechanism. (a) Side view drawing showing how the spherical shape is formed. (b) 3-D model in starting, intermediate, and final position (left-to-right). The inner diameter of the quarter-spheres shown here is 20 mm.

thickness using a flat blade guided by spacers on either side of the surface. The thickness of the pre-coated layers is verified to within 0.15 mm with a LK-H022 laser displacement sensor from Keyence Corporation. A Vision Research Phantom Miro eX4 Color high speed camera was used to record impact events with a 50 mm lens at aperture f5.6, at an image resolution of  $512 \times 512$  pixels and a sampling rate of 2000 frames/s.

A mirror at a  $45^\circ$  angle beneath the glass plate allows the camera to capture a biaxial view of the impact event. The combination of the side view and bottom view gives a more complete image of the impact, which is helpful in determining the type of impact event (see Figure 10).

### III. RESULTS

An annotated compilation of videos associated with the still images shown here can be found online at Ref. 20. One of the key features of yield-stress fluid drops is that upon impact they can stick to a surface. Of the myriad factors that can be measured and analyzed from the videos shown below, here we choose to examine this sticking behavior. Whether the drop sticks and the material stays localized or the drop splashes and the material is distributed is a fundamental characteristic of the impact event that is relevant to all droplet applications and provides a good starting point to understanding the physics at work. Figure 5 compares this sticking phenomenon with Newtonian behavior. The yield-stress fluid leaves a crater and a ring on the surface, showing halted motion and

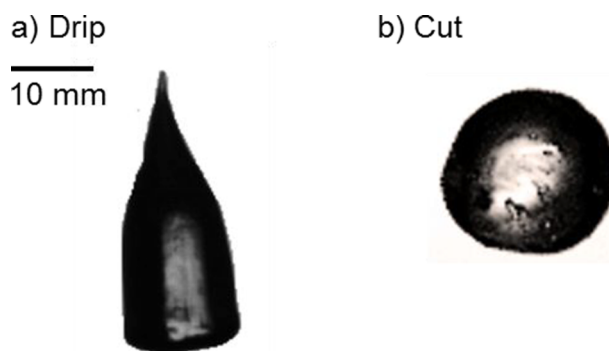


FIG. 3. Cutting mechanism performance. (a) Drop extruded from a syringe and formed by gravity; (b) drop cut by mechanism detailed in Figure 2.

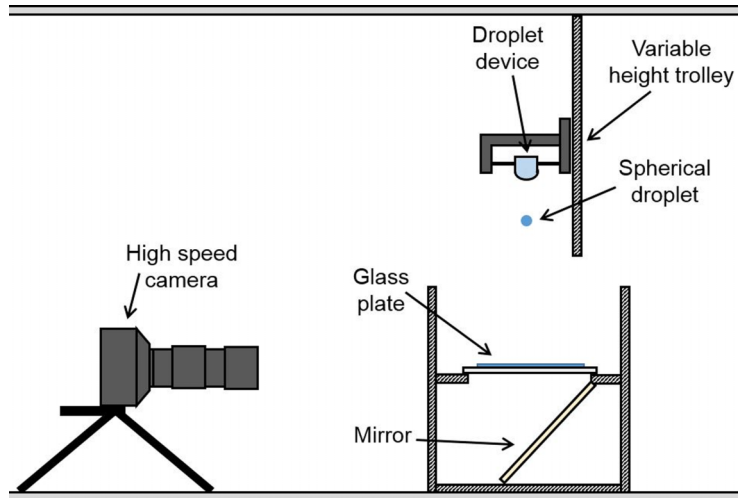


FIG. 4. Diagram of the high speed video apparatus (not shown to scale).

“sticking,” while the Newtonian fluid continually flows back to the impact site to eventually renew a flat surface.

The sticking phenomenon may halt drop impact dynamics at various points during the impact event, depending on the conditions. A typical impact event involves crater formation, sheet ejection, sheet breakup, and droplet formation. Figures 6–9 show high speed video images under different conditions, demonstrating a range of behaviors where motion is halted at different points of the impact event. Four parameters are varied: gel concentration, pre-coated layer thickness, impact velocity, and drop size. We will use the word “splashing” to refer to impact events that involve sheet breakup into multiple coherent volumes (droplet formation). These events tend to broadly spread material away from the impact location. When motion is halted earlier in the impact event, the drop tends to “stick” and stay near the impact location.

Figure 6 shows images at progressing time of three impact events at varying concentrations while holding constant the velocity, thickness, and drop size. As the concentration of the gel increases (increasing the yield stress of the material), the impact behavior transitions from splashing to sticking. The 0.1% gel forms a very large ejection sheet that ruptures and results in free droplets with high outward velocity. The 0.25% gel forms a smaller ejection sheet that experiences rupture, but the outward momentum is, nonetheless, halted and the material spreading is limited. The 1.0% gel is one cohesive mass throughout the event, and no material escapes a small radius around the center of impact.

These impacts show several other features that are not seen in Newtonian fluids. In all three cases in Figure 6, the impact crater stops expanding. In Newtonian droplets, the expanding extent of flow in the base layer can slow due to viscous forces but never completely stops during the impact event. The presence of a yield stress causes expansion of the disturbance in the base layer to halt when the flow stresses in the crater fall below the yield stress. The images show that in the higher concentration drops, the base pins sooner and closer to the center of the impact event. This results in a shallower angle between the ejection sheet and the surface as the yield stress increases. A Newtonian fluid will also evolve to spherical droplets and flat surfaces due to capillary forces given sufficient time. The ability of the yield stress to outweigh capillary stresses allows the Carbopol to hold irregular shapes at the end of the impact event. The 0.1% gel shows thread-like strands at 0.1 s, the 0.25% gel shows a suspended ribbon-like ring at 0.1 s, and the 1.0% gel holds a crater after 0.05 s. The frames at 0.01 s also show an increase in smoothness and a decrease in crowning around the top of the ejection sheet as the concentration increases.

Figure 7 shows three impacts onto pre-coated layers with varying thicknesses (drop size, velocity, and material concentration are held constant). The transition from splash to stick occurs as the pre-coating layer thickness increases. When the thickness is high, the material remains cohesive and

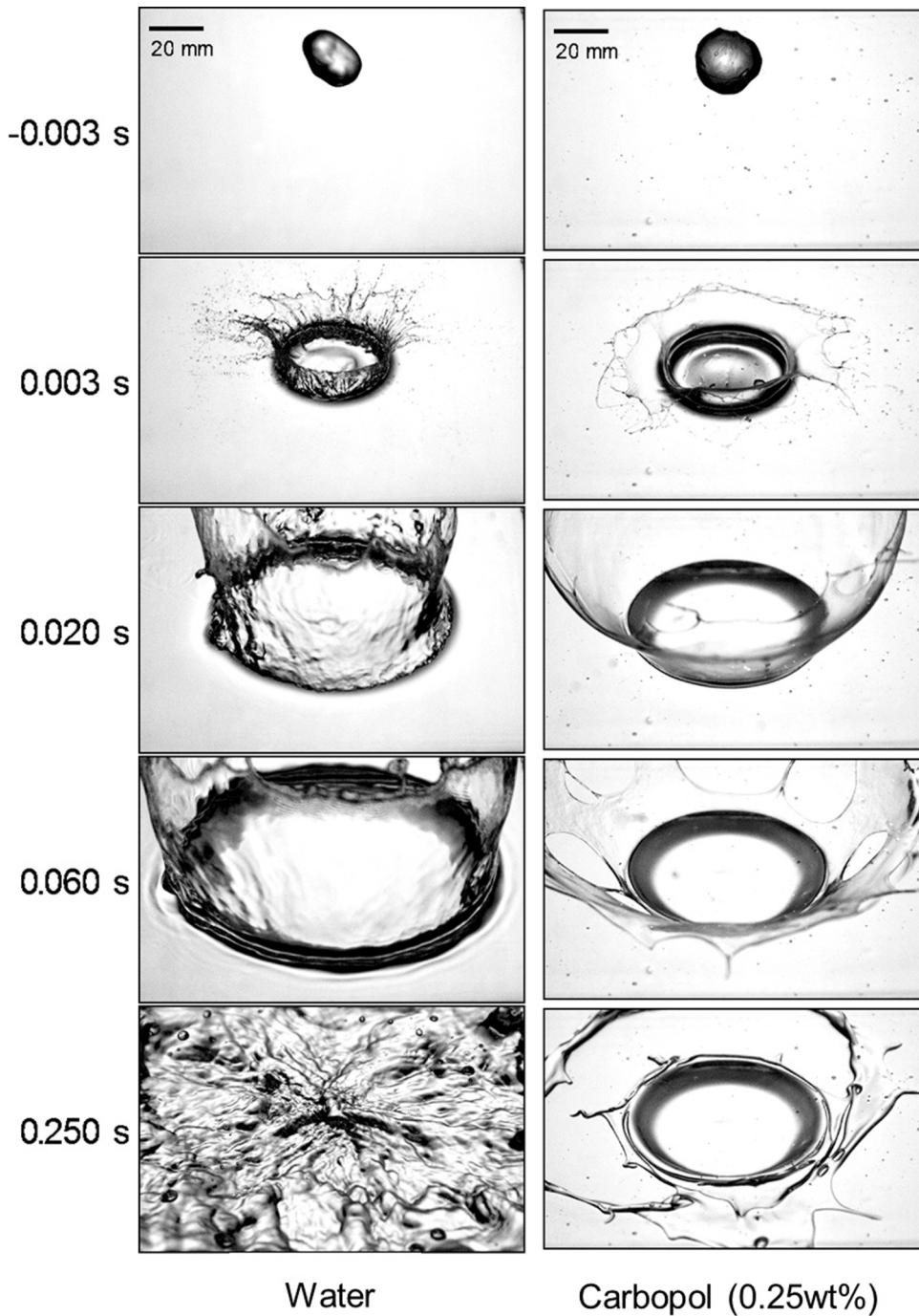


FIG. 5. Comparison of water and a yield-stress fluid (aqueous Carbopol). Water continually flows, whereas Carbopol holds a crater and a ring. Drops of 20 mm diameter impacting a 4 mm thick layer at 5.5 m/s.

no droplets are ejected, while at lower thicknesses, the ejection sheet breaks up and droplets leave with high outward momentum. The angle between the ejection sheet and the surface also varies, getting steeper with more prominent “stick” as the thickness increases. Note that this is the reverse trend from what was seen when concentration is varied; there material sticks when the ejection angle is low (Figure 6, 0.01 s). In Figure 7, at all thicknesses, the shape of the ejection sheet is the same (conical), whereas in Figure 6, the sheet shows a change in curvature as the concentration varies. The duration of the impact event from first contact to all materials coming to rest is roughly

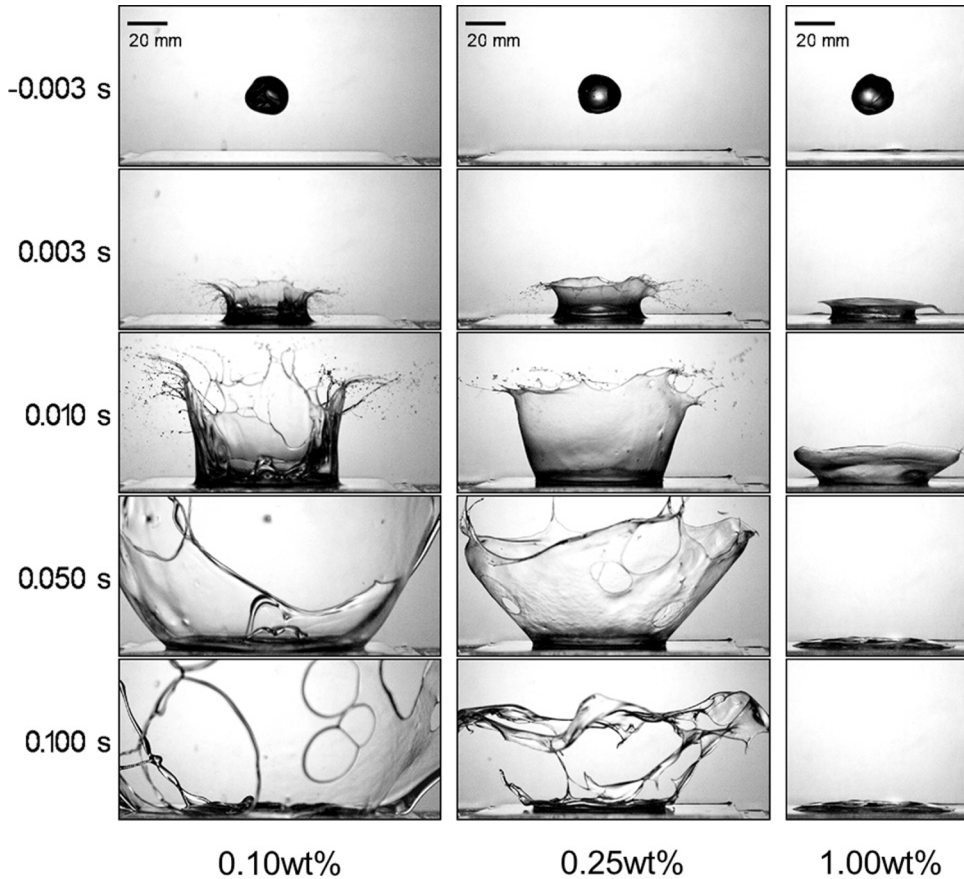


FIG. 6. Varying concentrations: 20 mm diameter drops impacting a 4.0 mm thick layer of material at 6.3 m/s.

constant with varying thicknesses (the event is longer when the layer is thinner, but the difference in time is small in Figure 7), whereas with varying concentrations, this timescale varies greatly (Figure 6). We will also see the same timescale varying with velocity and initial drop size.

Figure 8 shows three impacts at varying velocities, while holding constant the drop size, layer thickness, and concentration. The transition from stick to splash occurs as the impact velocity increases. At 2.5 m/s, the event is very short (all motion stopped within 0.02 s), and no material travels more than 30 mm from the center of impact. At 3.6 m/s, a straight-sided sheet forms and begins to break up, but all momentum is arrested before any droplets are produced. At 6.4 m/s, a large bowl-shaped sheet forms and explodes into an assortment of threads that spread outward.

Figure 9 shows three impacts at varying drop sizes with velocity, thickness, and concentration held constant. The transition from stick to splash occurs as the drop size increases. The 10 mm drop forms a straight-sided ejection sheet that reaches a maximum radial extent (at roughly 0.008 s), then retracts inward (as can be seen by the smaller final radius at 0.02 s and also in the video compilation<sup>20</sup>). The 15 mm drop forms a straight-sided sheet that ruptures from the middle, leaving a broken ring of material lying on the surface surrounding the impact area. The 25 mm drop forms a curved sheet that breaks up into threads that are ejected outwards.

In all four parameter variations (Figures 6–9), larger ejection sheets with greater curvature and longer impact event duration were associated with splashing, while straight-sided sheets and short timescales were associated with sticking, and motion being halted earlier in the impact event. The angle of the ejecting sheet varied with all four input parameters, but there was no consistent trend of splashing events corresponding to higher or lower angles compared to sticking events.

These videos demonstrate that a spectrum of behavior exists in the transition from sticking to splashing. To capture this, we classify the type of event according to five different categories: lump, crater, intact sheet, broken sheet, and splash. These categories correspond to how early or

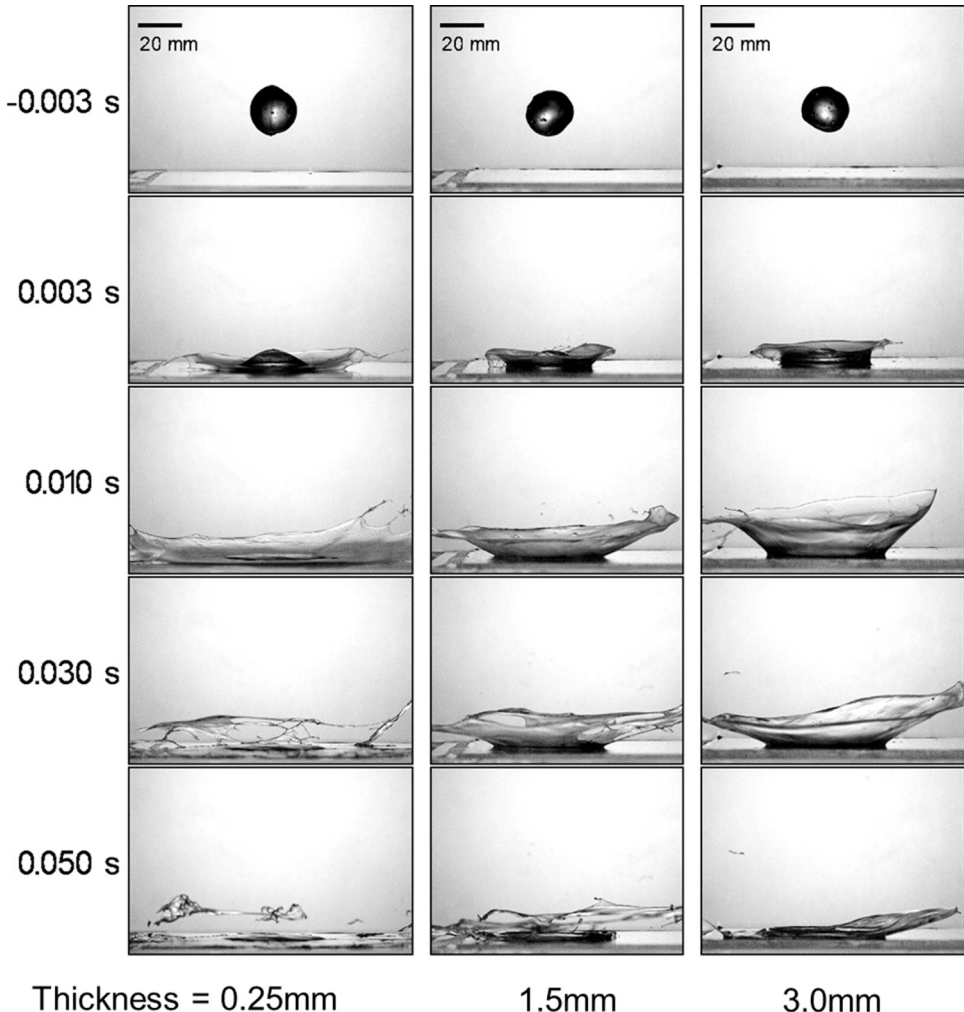


FIG. 7. Varying thicknesses of pre-coated layer. Drops of 20 mm of 0.5% Carbopol impacting at 5.6 m/s.

late the motion is halted during an impact event. These descriptive categories define an event as follows: a “lump” when the maximum height of the final profile lies at the center of the impact; a “crater” when the maximum height of the final profile lies away from the center of the impact and a sheet extending above the pre-coating (ejection sheet) does not form; an “intact sheet” when an ejection sheet forms but experiences no rupture; a “broken sheet” when the ejection sheet ruptures, but remains one contiguous mass; and a “splash” when the ejection sheet breaks into more than one piece.

We expect to see a transition from “lump” to “splash” behavior as input momentum increases and dissipative forces decrease. Greater drop diameter and impact velocity increase the input momentum, while lower concentration and thinner pre-coating thickness decrease dissipative forces. Therefore, splashing events (“splash” and “broken sheet”) are expected at large velocity, large diameter, low concentration, and small thickness, while sticking events (“lump,” “crater,” and “intact sheet”) are expected at small velocity, small diameter, high concentration, and large thickness. We performed tests at four values of each of these four parameters, as delineated in Table I, resulting in 256 distinct combinations of parameters. Values of yield stress and infinite-shear viscosity are attained from Bingham model fits of the data shown in Figure 1 (yield stress and infinite-shear viscosity are not varied independently, as they are determined by concentration). As we will see, this covers the parameter space to produce the range of behavior from “lump” to “splash,” including the examples shown in Figures 6–9.

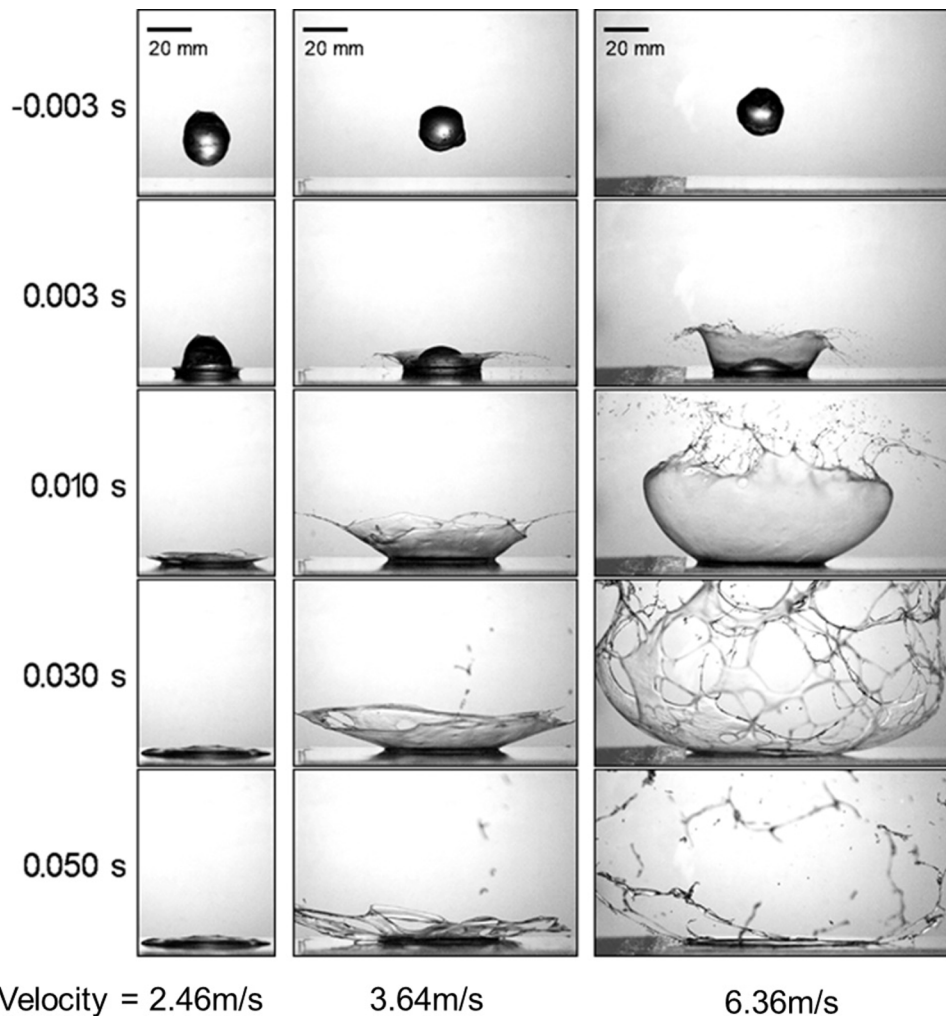


FIG. 8. Varying velocities. 20 mm diameter drops of 0.25% Carbopol impacting a 1.5 mm thick layer.

Uncertainties for velocity and diameter come from image analysis of the high-speed videos. Yield stress and infinite-shear viscosity variations are a combination of fit uncertainty and rheometer measurement repeatability. Thickness uncertainty comes from measurement with a laser-displacement meter.

Figure 10 is a two-dimensional grid of two-dimensional subplots, which maps the four-dimensional parameter space. At each coordinate location, a color-coded box indicates the type of impact as lump, crater, intact sheet, broken sheet, or splash. Each subplot has Cartesian coordinates of pre-coating thickness and drop diameter; a single subplot is associated with a fixed concentration and impact velocity. The subplots are organized as a grid with Cartesian coordinates corresponding to the concentration and velocity.

The regime map shows the expected extremes, converging to splash impacts in the upper left and lump impacts in the lower right of Figure 10. The transition is mostly monotonic between the event categories with respect to all four varied inputs. Moving both within each subplot and from subplot to subplot, sticking behavior is observed lower and farther to the right, while splashing behavior is observed higher and farther to the left. The transitions are smoothly resolved for the parameter values. Nowhere does one step in any parameter cause a transition of more than two categorizations, e.g. a crater never becomes a splash by increasing/decreasing one parameter by one increment in our experimental space (Table I).

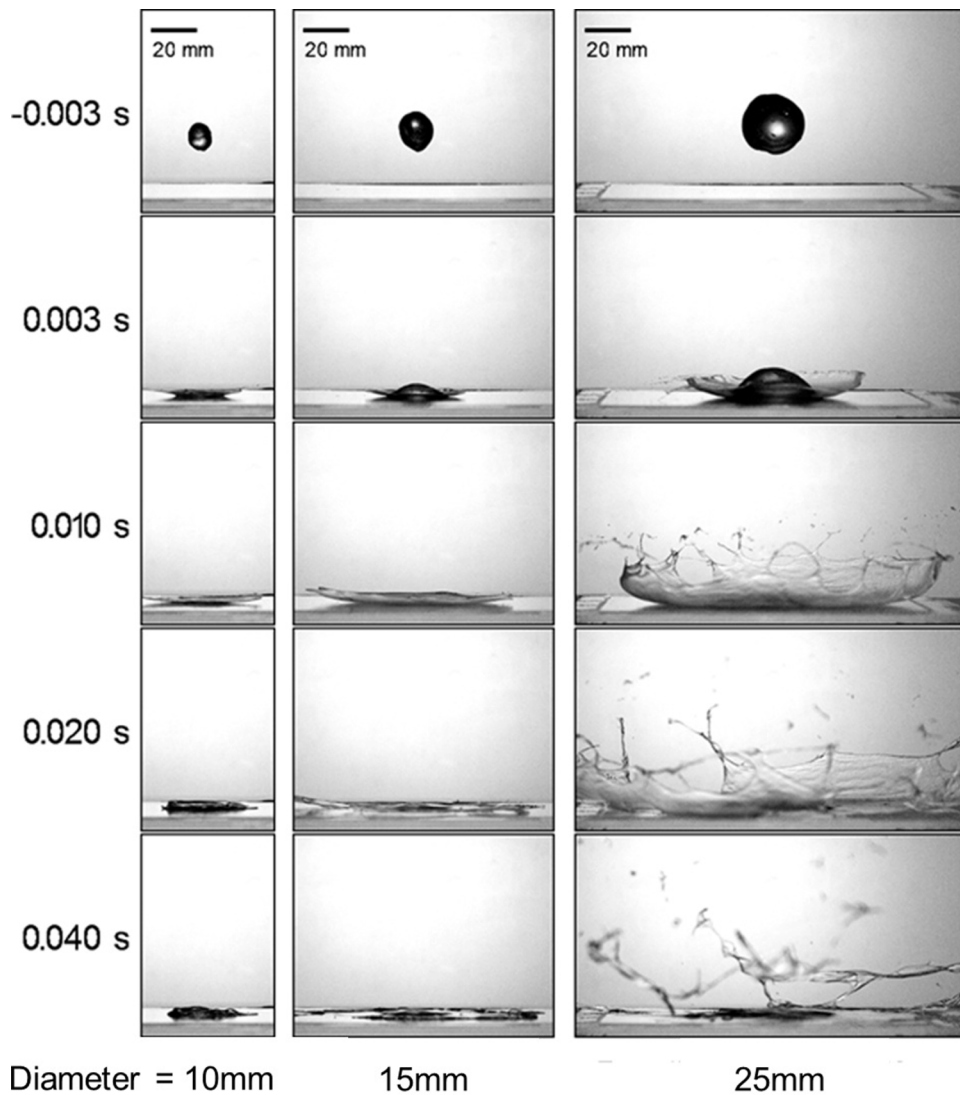


FIG. 9. Varying drop sizes. Drops of 0.5% Carbopol impacting a 0.5 mm thick layer at 4.9 m/s.

The wide range of observations in Figure 10 shows clear trends and lends understanding of the behavior. Yet, the four-dimensional parameter space would be complex for any application, especially those outside the specific range of values studied here. Next, we pursue dimensionless groups that (i) reduce the dimensionality from four parameters to as few as possible, ideally to one parameter; (ii) provide deeper insight into the physics; and (iii) potentially allow for extrapolation

TABLE I. Values of experimental parameters explored.

Parameter	Values tested			
Velocity ( $\pm 0.03$ m/s)	2.54	3.81	5.09	6.35
Concentration (wt. %)	0.10	0.15	0.25	1.00
Yield stress ( $\pm 2$ Pa)	13	33	64	106
Infinite-shear viscosity ( $\pm 0.05$ Pa s)	0.23	0.49	0.96	2.10
Diameter ( $\pm 0.2$ mm)	10	15	20	25
Thickness ( $\pm 0.15$ mm)	0.5	1.5	3.0	4.0

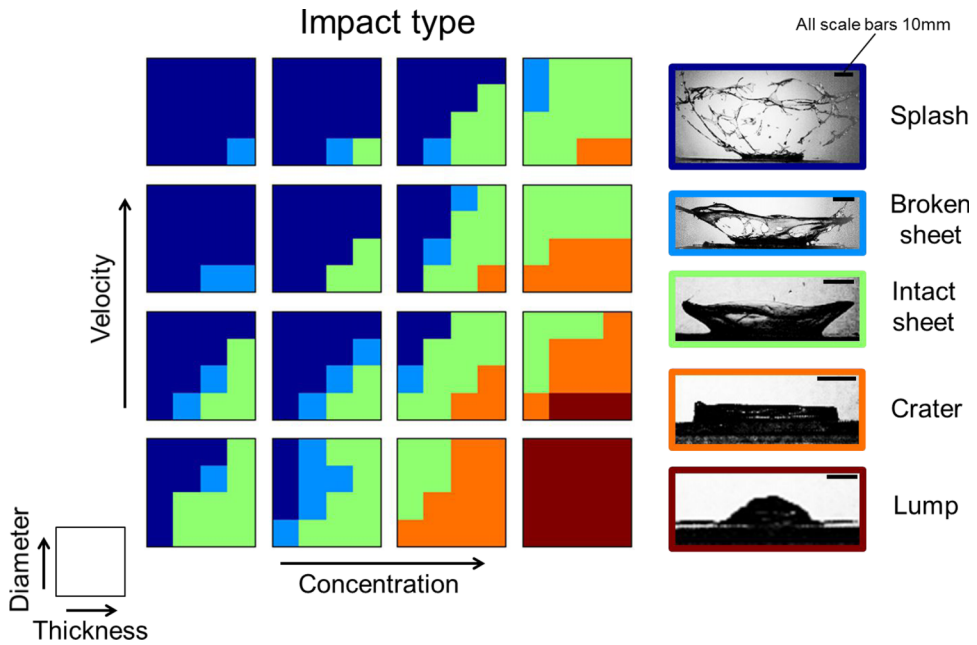


FIG. 10. Impact type plotted as a function of four dimensional input parameters. Values of velocity, concentration, diameter, and thickness are shown in Table I.

of these results beyond the range of parameters explicitly explored here, in cases with dynamic and geometric similarities to the experiments performed here.

#### IV. DIMENSIONLESS GROUPS

Our goal is to reduce the number of parameters required to characterize this space, ideally identifying a single parameter that indicates the type of impact event a drop will exhibit. Prior work found good results separating splash and deposition in Newtonian droplets impacting thin films using a combination of the Weber number

$$\text{We} = \rho V^2 D / \gamma, \quad (1)$$

Ohnesorge number

$$\text{Oh} = \eta / \sqrt{\rho \gamma D}, \quad (2)$$

and dimensionless film thickness  $t/D$  (Figure 10 of Ref. 9), where  $\gamma$  is the surface tension. Figure 11 shows a plot of the parameter used by Ref. 9 using  $\eta_\infty$  in place of  $\eta$  in Eq. (2).

For Newtonian fluids, a transition from deposition to splash was seen for values of the calculated parameter greater than one (shown as a dashed line in Figure 11). In contrast to the Newtonian result, the yield stress data in Figure 11 show a stronger tendency toward deposition (exhibiting deposition at higher values of the parameter) and also a larger region of the parameter space where both sticking and splashing events occur. The greater overlap between the behavioral regimes indicates that this correlation is not effectively applicable to yield-stress drops.

For further analysis, we consider the output as a function of seven parameters: four fluid properties (yield stress, infinite shear viscosity, surface tension, and density), two geometric (drop diameter and pre-coating layer thickness), and one flow (impact velocity). Other parameters, such as thixotropic timescale and extensional viscosity, may also affect the dynamics. At present, we omit these because the thixotropic restructuring time is not likely to vary in our experiments (changing the material to change this timescale stands as interesting future work), and variation in extensional viscosity in Carbopol is not substantially different than variation in shear viscosity.<sup>21</sup> It is worth noting that measurement of surface tension in yield-stress fluids is a challenging task, as the presence

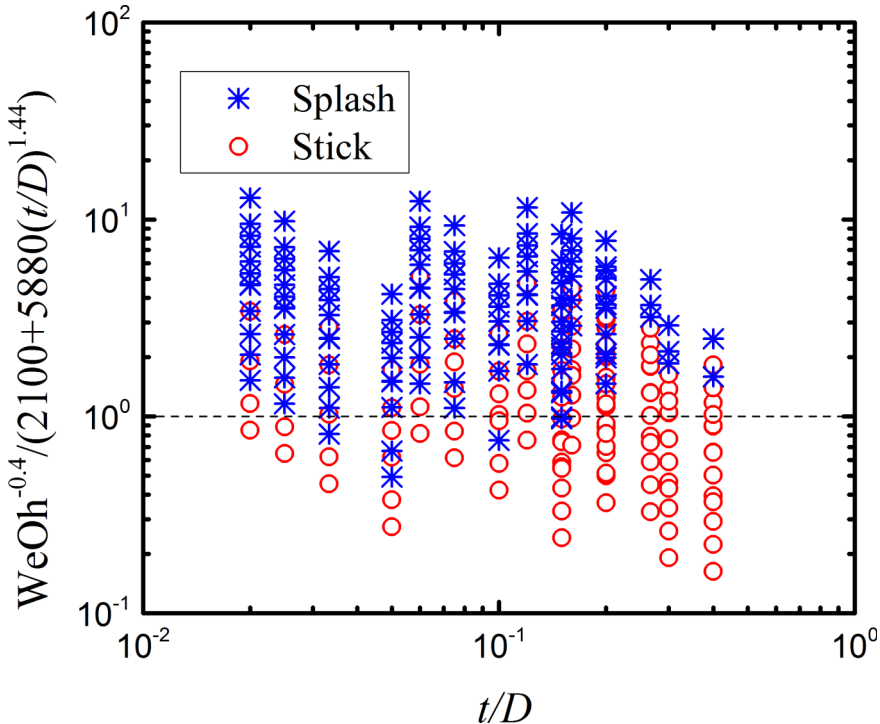


FIG. 11. Correlation for Newtonian droplets does not perform well for yield-stress drops. We and Oh are defined in Eqs. (1) and (2), respectively.

of a yield stress invalidates many common methods of quantifying capillary forces. Recent work measuring the surface tension of Carbopol found that its deviation from that of water was small (less than 10%), and that it did not vary strongly with gel concentration.<sup>22</sup>

By the Buckingham Pi theorem, the independent parameter space (seven parameters) can be characterized by a maximum of four dimensionless groups. A number of dimensionless groups have already been examined in the literature for impacts of yield-stress drops onto dry surfaces (e.g., Table II of Ref. 23). It can easily be seen from Figures 6–9 that the thickness of the pre-coating layer has a non-negligible effect; hence, the previously outlined groups<sup>23</sup> prove insufficient when trying to distinguish between impact regimes on coated surfaces.

We now construct a new dimensionless group beginning with the hypothesis that the stick-to-splash transition will best be governed by a comparison of inertia to dissipative flow forces (the latter involving both the yield stress and rate-dependent viscous forces). The presence of two length scales in the problem requires judicious choices as to when the use of drop diameter  $D$  or coating thickness  $t$  is appropriate. We calculate the characteristic inertial, yield, and viscous stresses as

$$\text{Inertial stress} = \rho V^2, \quad (3)$$

$$\text{Yield stress} = \sigma_y, \quad (4)$$

$$\text{Viscous stress} = \eta_\infty V/t, \quad (5)$$

respectively.

Table II shows the minimum and maximum values of each of these stresses that are covered in our experimental space. Note that the shown minima and maxima are the values from initial conditions and represent an aggregate single value for each test; higher and lower stresses exist at specific times or locations within each impact event.

The use of  $t$  as the lengthscale in the viscous stress is appropriate under the assumption that flow permeates the impacting layer. The velocity at the surface scales with the impacting velocity, hence the appropriate scaling for the characteristic shear rate is  $V/t$  if the velocity gradient is constant throughout the layer. The videos for all but a few of our tests (those with the smallest

TABLE II. Range of stresses covered in our experimental space, from Eqs. (3)–(5).

Stress	Minimum (Pa)	Maximum (Pa)
Inertial	6450	40 300
Yield	13	106
Viscous	146	26 700

diameters and largest pre-coating thicknesses, ~10% of the trials) show that this assumption is good. If conditions were such that the flow did not permeate the layer, and the location of zero velocity was the edge of an unyielded portion of the fluid rather than the boundary, another length-scale would be more appropriate (e.g. in the semi-infinite limit, velocity gradient lengthscale would have no dependence on the thickness). The dimensionless group comparing inertial stress ( $I$ ) to flow stress ( $F$ ) then takes the form,

$$IF = \frac{\rho V^2}{\sigma_y + \eta_\infty V/t} \sim \frac{\text{inertial stress}}{\text{flow stress}}. \quad (6)$$

The geometry of the problem dictates that we consider balance of forces rather than stresses to appropriately incorporate all length scales. Figure 12 shows an image of a droplet impact with a mirror beneath the clear impact surface, giving a side view and an underneath view of the crater and ejection sheet.

Drawn on this are shapes showing how the relevant areas in the problem scale with the two length scales that we are examining. We convert the stresses in Eq. (6) to forces by multiplying by appropriate areas, considering that inertial stresses should convert to forces by the area  $\sim D^2$ , and viscous and yield stresses should convert to forces by the area  $\sim D \times t$ . The ratio of inertial forces to dissipative flow forces is then approximated by

$$\frac{\rho V^2 D}{(\sigma_y + \eta_\infty V/t) t} = IF \frac{D}{t} \sim \frac{\text{inertial force}}{\text{flow force}}. \quad (7)$$

We hypothesize that constant values of this force ratio identify transitions between impact regimes. In other words, this predicts that the critical regime transition scales as

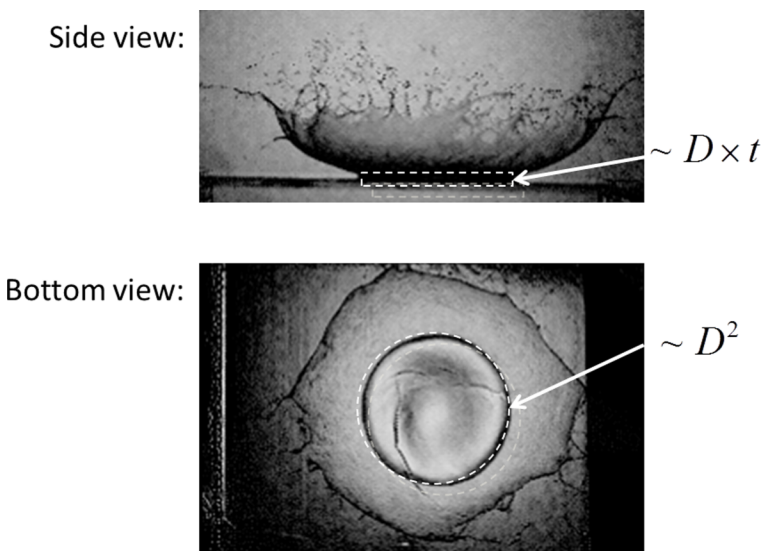


FIG. 12. Image shows lengthscales used in scaling arguments, which is how pre-coating thickness is incorporated into the analysis. Forces from stresses that act over the area of the crater are scaled by the drop diameter squared, while forces from stresses that act over the area of the ejecting sheet scale like the product of drop diameter and layer thickness.

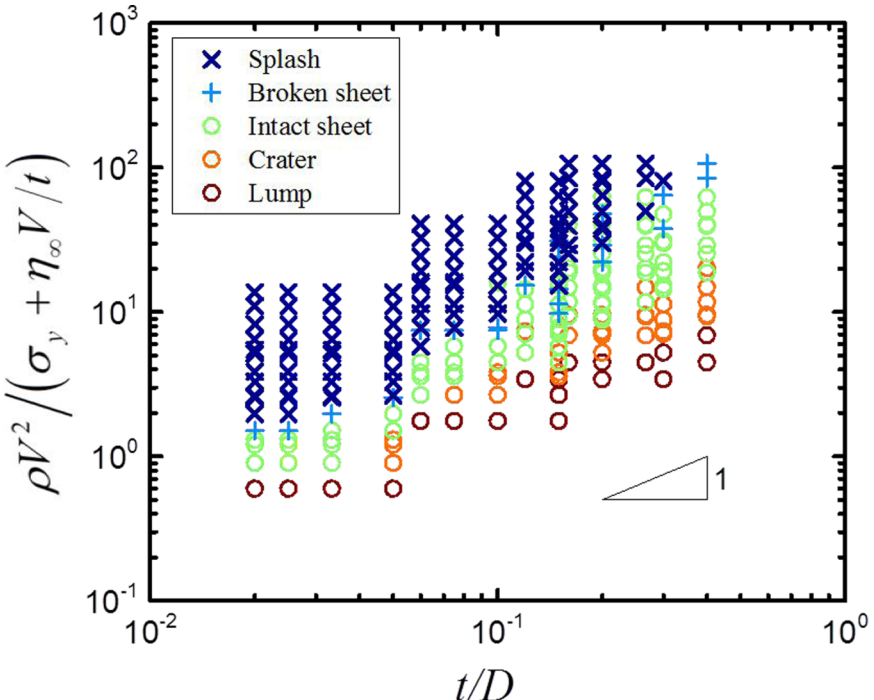


FIG. 13. Ratio of inertia to dissipative flow stress effectively separates impact regimes across all values of thickness. A boundary with double-log slope of one is predicted by Eq. (8).

$$\frac{\rho V^2}{\sigma_y + \eta_\infty V/t} \sim \frac{t}{D}. \quad (8)$$

To test this hypothesis, Figure 13 shows a regime map of the impact type, plotted with dimensionless layer thickness ( $t/D$ ) on the abscissa and IF on the ordinate.

This framing does a much better job of separating the different types of impact behavior compared to Figure 11. At smaller values of  $\frac{\rho V^2 D}{(\sigma_y + \eta_\infty V/t)t}$  (when the dissipative flow force is greater than the inertial force), we see sticking behavior, and at larger values of  $\frac{\rho V^2 D}{(\sigma_y + \eta_\infty V/t)t}$  (when the inertial force is greater than the dissipative flow force), we see splashing behavior. As predicted in Eq. (8), the transitions between regimes show a slope of approximately 1.

At the lowest and highest values of  $t/D$  examined, separation between regimes is perfect with no overlap (no range of values of IF for which one impact type is observed contains instances of another impact type). At moderate  $t/D$ , a small amount of overlap is present, but stick events and splash events never coincide for more than a half decade of values of IF. This is greatly improved over the regime map shown in Figure 11, which shows over a decade of overlap between stick and splash events, and superior to the other parameters we explored (including combinations of Reynolds, Ohnesorge, and capillary numbers).

It is worth noting that in this study, we have not varied the yield stress and the infinite shear viscosity independently. The ratio  $\sigma_y/\eta_\infty$  is roughly the same for each of the four concentrations of Carbopol that we used. Therefore, the data points characterized by a higher yield stress also inherently have higher viscous dissipation. Separately varying the yield stress and infinite shear viscosity stands as future work. This could be done by testing different materials with identical yield stress but varying infinite shear viscosities.

## V. CONCLUSIONS

Here, we experimentally observe drops of yield-stress fluid impacting pre-coated surfaces and study key features that the presence of a yield stress enables: the ability to stick to a surface, inhibit

splash, and form a lump or crater. Impacts onto pre-coated surfaces exhibit many features that are not observed on dry surfaces, most importantly, the formation of large long-lifetime ejection sheets with redirected momentum which extend away from the impact location. Yield-stress droplets also show many features that are not present in Newtonian droplet impacts, most importantly, the ability to stick and hold odd shapes.

By varying the drop size, impact velocity, pre-coating layer thickness, and material concentration, we demonstrate that the transition from splashing to sticking occurs with decreasing input momentum (decreasing velocity and drop size) and increasing dissipation (increasing concentration and thickness). In examining the nondimensionalization, we demonstrate that existing dimensionless groups do not adequately characterize the problem. By adjusting the definitions to properly incorporate yield stress effects and the new length scale of the pre-coating thickness, we show that the ratio of the inertial forces to flow forces, calculated as  $\frac{\rho V^2}{\sigma_y + \eta_\infty V/t} \left(\frac{D}{t}\right)$ , can identify regimes of stick/splash behavior. This single parameter reduces the dimensionality of the space one must examine to determine droplet dynamics, lends insight into the physics of the impact problem, and potentially allows for extrapolation of these results to dynamically and geometrically similar situations beyond the explicit material and parameter values explored here.

## ACKNOWLEDGMENTS

This work was supported by the National Science Foundation under Grant No. CBET-1351342 and the University of Illinois at Urbana-Champaign under the Interdisciplinary Innovation Initiative (In3) program.

- <sup>1</sup> N. J. Balmforth, I. A. Frigaard, and G. Ovarlez, "Yielding to stress: Recent developments in viscoplastic fluid mechanics," *Annu. Rev. Fluid Mech.* **46**, 121–146 (2014).
- <sup>2</sup> S. Nigen, "Experimental investigation of the impact of an (apparent) yield-stress material," *Atomization Sprays* **15**, 103–117 (2005).
- <sup>3</sup> L.-H. Luu and Y. Forterre, "Drop impact of yield-stress fluids," *J. Fluid Mech.* **632**, 301–327 (2009).
- <sup>4</sup> G. German and V. Bertola, "Impact of shear-thinning and yield-stress drops on solid substrates," *J. Phys.: Condens. Matter* **21**, 375111 (2009).
- <sup>5</sup> S. Rahimi and D. Weihs, "Gelled fuel simulant droplet impact onto a solid surface, Propellants, explosives," *Pyrotechnics* **36**, 273–281 (2011).
- <sup>6</sup> E. Kim and J. Baek, "Numerical study of the parameters governing the impact dynamics of yield-stress fluid droplets on a solid surface," *J. Non-Newtonian Fluid Mech.* **173-174**, 62–71 (2012).
- <sup>7</sup> M. Guémas, Á. G. Marín, and D. Lohse, "Drop impact experiments of non-Newtonian liquids on micro-structured surfaces," *Soft Matter* **8**, 10725 (2012).
- <sup>8</sup> M. Rein, "The transitional regime between coalescing and splashing drops," *J. Fluid Mech.* **306**, 145–165 (1996).
- <sup>9</sup> G. E. Cossali, A. Coghe, and M. Marengo, "The impact of a single drop on a wetted solid surface," *Exp. Fluids* **22**, 463–472 (1997).
- <sup>10</sup> A.-B. Wang and C.-C. Chen, "Splashing impact of a single drop onto very thin liquid films," *Phys. Fluids* **12**, 2155 (2000).
- <sup>11</sup> D. Sivakumar and C. Tropea, "Splashing impact of a spray onto a liquid film," *Phys. Fluids* **14**, L85–L88 (2002).
- <sup>12</sup> C. Josserand and S. Zaleski, "Droplet splashing on a thin liquid film," *Phys. Fluids* **15**, 1650 (2003).
- <sup>13</sup> R. L. Vander Wal, G. M. Berger, and S. D. Mozes, "The splash/non-splash boundary upon a dry surface and thin fluid film," *Exp. Fluids* **40**, 53–59 (2005).
- <sup>14</sup> R. L. Vander Wal, G. M. Berger, and S. D. Mozes, "Droplets splashing upon films of the same fluid of various depths," *Exp. Fluids* **40**, 33–52 (2005).
- <sup>15</sup> R. Rioboo, C. Bauthier, J. Conti, M. Voue, and J. De Coninck, "Experimental investigation of splash and crown formation during single drop impact on wetted surfaces," *Exp. Fluids* **35**, 648–652 (2003).
- <sup>16</sup> G. E. Cossali, M. Marengo, A. Coghe, and S. Zhdanov, "The role of time in single drop splash on thin film," *Exp. Fluids* **36**, 888–900 (2004).
- <sup>17</sup> J. Labanda, P. Marco, and J. Llorens, "Rheological model to predict the thixotropic behaviour of colloidal dispersions," *Colloids Surf., A* **249**, 123–126 (2004).
- <sup>18</sup> R. H. Ewoldt, M. T. Johnston, and L. M. Caretta, "Experimental challenges of shear rheology: How to avoid bad data," in *Complex Fluids in Biological Systems*, edited by S. Spagnolie (Springer, 2015).
- <sup>19</sup> C. W. Macosko, *Rheology Principles, Measurements, and Applications* (Wiley, New York, 1994).
- <sup>20</sup> B. C. Blackwell, M. E. Deetjen, J. E. Gaudio, and R. H. Ewoldt, "Liquid-solid impacts of yield-stress fluids," APS-DFD Gallery of Fluid Motion (APS-DFD, 2013); e-print [arXiv:1310.4186](https://arxiv.org/abs/1310.4186).
- <sup>21</sup> G. German and V. Bertola, "Formation of viscoplastic drops by capillary breakup," *Phys. Fluids* **22**, 033101 (2010).
- <sup>22</sup> J. Boujlel and P. Coussot, "Measuring the surface tension of yield stress fluids," *Soft Matter* **9**, 5898 (2013).
- <sup>23</sup> A. Saïdi, C. Martin, and A. Magnin, "Influence of yield stress on the fluid droplet impact control," *J. Non-Newtonian Fluid Mech.* **165**, 596–606 (2010).